



Published in final edited form as:

Obstet Gynecol. 2005 December ; 106(6): 1259–1265.

Magnetic Resonance Imaging and 3-Dimensional Analysis of External Anal Sphincter Anatomy

Yvonne Hsu, MD, Dee E. Fenner, MD, William J. Weadock, MD, and John O. L. DeLancey, MD
From the Pelvic Floor Research Group and Division of Gynecology, Department of Obstetrics and Gynecology and Department of Radiology, University of Michigan, Ann Arbor, Michigan.

Abstract

OBJECTIVE: To use magnetic resonance images of living women and 3-dimensional modeling software to identify the component parts and characteristic features of the external anal sphincter (EAS) that have visible separation or varying origins and insertions.

METHODS: Detailed structural analysis of anal sphincter anatomy was performed on 3 pelvic magnetic resonance imaging (MRI) data sets selected for image clarity from ongoing studies involving nulliparous women. The relationships of anal sphincter structures seen in axial, sagittal, and coronal planes were examined using the 3-D Slicer 2.1b1 software program. The following were requirements for sphincter elements to be considered separate: 1) a clear and consistently visible separation or 2) a different origin or insertion. The characteristic features identified in this way were then evaluated in images from an additional 50 nulliparas for the frequency of feature visibility.

RESULTS: There were 3 components of the EAS that met criteria as being “separate” structures. The main body (EAS-M) is separated from the subcutaneous external anal sphincter (SQ-EAS) by a clear division that could be observed in all (100%) of the MRI scans reviewed. The wing-shaped end (EAS-W) has fibers that do not cross the midline ventrally, but have lateral origins near the ischiopubic ramus. This EAS-W component was visible in 76% of the nulliparas reviewed.

CONCLUSION: Three distinct external anal sphincter components can be identified by MRI in the majority of nulliparous women.

Obstetric sphincter injury and fecal incontinence can be a devastating problem for recently parturient women. The advent of modern imaging has allowed us to determine the presence or absence of anal sphincter injury and revolutionized our understanding of anal incontinence. As many as 35% of primiparous women sustain anal sphincter injuries during vaginal delivery, and these injuries have been correlated with fecal incontinence and other bowel symptoms.¹ Although clinical observations highlight the importance of the anal sphincter to the continence mechanism, knowledge of the anal sphincter anatomy is limited.

Significant controversy exists about the number of component parts contained in the external anal sphincter (EAS) based on cadaveric dissection. Dalley² reviewed the various descriptions of EAS anatomy and found reports of 2, 3, or 4 parts in the literature. With improvements in magnetic resonance (MR) imaging, it has become possible to study the fine detail of the anal sphincter complex in living women.^{3,3} This avoids the artifactual problems that arise through the process of dissection as well as the considerable problem of finding reproductive age specimens without potential birth damage to dissect. In this study we sought to use MR imaging

Corresponding author: Yvonne Hsu, 1500 E. Medical Center Dr., Women’s Hospital L4000, University of Michigan, Ann Arbor, MI, 48109-0276; yvonneh@med.umich.edu, Phone: 734.764.8429, Fax: 734.647.9727.

Supported by National Institutes of Health through the Office for Research on Women’s Health SCOR on Sex and Gender Factors Affecting Women’s Health With funding From NICHD P50 HD044406.

and 3-dimensional modeling to evaluate the number of visible components of the external anal sphincter. The ability to divide the external anal sphincter into components allows correlation of specific defects to alterations in function.

MATERIALS AND METHODS

Magnetic resonance scans of the anal sphincter in nulliparous women from 3 ongoing institutional review board–approved studies were used in this project. There were 2 phases of the study: 1) structural analysis and model creation using 3 MR scans and 2) evaluation of how often characteristic features found in phase 1 of the study can be seen in 50 additional MR scans.

The nulliparous MR scans used in this project were selected from an existing library composed of scans from 3 institutional review board–approved studies. All MR sequences were obtained in the supine position with a body coil. Multiplanar 2-dimensional proton density pelvic MR images (time of echo 15 ms, time of repetition 4,000 ms) were obtained by use of a 1.5 T superconducting magnet (Signa Horizon LX, General Electric, Milwaukee, WI). The field of view in axial and coronal images were both 16 cm × 16 cm and in the sagittal images 20 cm × 20 cm. All 3 acquisitions had a slice thickness of 4 mm, with 1 mm gap between slices.

In phase 1, preliminary analysis was performed to develop criteria for subdivision identification and to create a 3-dimensional model. Detailed slice-by-slice examinations of axial, sagittal, and coronal images were conducted using 3 nulliparous MR studies (ages 25, 32, and 37 years). These studies were selected for the clarity of the anal sphincter anatomy. The original source Digital Imaging and Communications in Medicine MR data were used and consisted of a series of images. The subdivisions of the external anal sphincter were traced in each slice and then connected together by the 3-D slicer 2.1b1 program (Massachusetts Institute of Technology Artificial Intelligence Laboratory and the Surgical Planning Laboratory at Brigham and Women’s Hospital, Boston, MA) to create a 3-dimensional volume. The program displays data in all 3 orthogonal planes. This allowed the appearance of a structure seen in 1 scan plane (eg, axial) to be related to structures seen in another plane (eg, sagittal) by having all 3 orthogonal planes in the same 3-dimensional space. For each component of the EAS, tracings and 3-dimensional models were made in all 3 scan planes. Tracing of the structures and 3-dimensional models were reviewed independently by 2 examiners. Each 3-dimensional model was validated by overlaying the model with the original source image. Characteristic features of the EAS components in each scan plane were catalogued.

We used the following criteria to determine whether 1 element in the sphincter should be considered separate from the other elements: 1) visible separation between 1 element and adjacent structures or 2) differing origin or insertion of the muscle. These same criteria were used in the second phase of the study.

In phase 2, a convenience sample of 50 MR scans of nulliparous women were reviewed to see how often the characteristic features of the sphincter could be identified. These scans were taken from an existing library of women recruited as part of 3 different studies on pelvic organ support and urinary incontinence. Our past anatomic experience has shown that 50 subjects is an adequate sample to reveal common anatomic variations. Women were recruited through newspaper advertisements, bulletins, “word-of-mouth,” and using the Michigan Health Registry, a list of women willing to be contacted for women’s health studies. Women were enrolled between November 1999 and February 2005. Women were excluded based on a clinical history of having more than rare episodes of liquid stool incontinence or any loss of solid stool. None of the women included for analysis had significant fecal incontinence.

RESULTS

There were 3 components of the external anal sphincter that met criteria for consideration as a separate structure. These are the main body (EAS-M), the winged portion (EAS-W) and the subcutaneous portion (SQ-EAS). The 3-dimensional model and the subdivisions of the external anal sphincter are shown in Figure 1. Figure 2 is a simplified drawing of the sphincter complex based on the 3-dimensional model. The cross-sectional anatomy of the external anal sphincter in the axial, coronal, and sagittal scan planes are shown in Figure 3, Figure 4, and Figure 5, respectively. Table 1 summarizes the characteristic sphincter features in the different scan planes and provides specific reference to the panels where they can be seen in the figures. Review of Table 1 and cross-sectional images seen in Figures 3, 4, and 5 with reference to the 3-dimensional model will allow the reader to assess the anatomic findings.

The axial plane most consistently demonstrates the 3 components. Ventrally, the main body of the EAS (EAS-M) can easily be distinguished lateral to the subcutaneous external anal sphincter (SQ-EAS) separated by a connective tissue space that we refer to as the external sphincter space (ESS, Fig. 3, panels -2.5 to 0. Note well that the ESS is not to be confused with the intersphincteric groove, which is the separation between the internal and external anal sphincters where the longitudinal muscle of the bowel and levator ani pass between these sphincters to reach the perineal skin and which is not well seen on MRI). It is possible to see the fibers of the EAS-M and the SQ-EAS cross the midline distinct from one another in this scan plane (Table 1 and Fig. 3), forming a double thickness of muscle. Dorsally, it is not possible to distinguish between the fibers of the EAS-M and the SQ-EAS as they decussate to the anococcygeal ligament (Fig. 3, panel -3.0). Also, the SQ-EAS on either side of the anal skin and the surrounding EAS form the shape of a “W,” causing the appearance of an invaginated complex (Fig. 3, panels -2.5 to -1.5).

It is in axial scan images that the wing-shaped EAS-W can be seen (Table 1 and Fig. 3, panels -2.0 to -1.0). It is possible to distinguish EAS-W from EAS-M because it contains fibers that flare out laterally, which do not cross the midline ventrally. Although there is not a visible separation between the fibers of the EAS-W and the EAS-M, the differences in fiber directions denote differing origins and insertions. The lateral fibers of the EAS-W usually have a clear separation from the adjacent fibers of the puborectalis muscle (Table 1 and Fig. 3, panels -2.0 and -1.5).

The addition of the coronal scan plane to the axial scan plane gives a much clearer picture of the 3-dimensional geometry of the external sphincter. Because of the oblique orientation of the sphincter, the ventral crossing fibers of the SQ-EAS and the EAS-M that can be distinguished in the axial plane appear as 1 structure on the coronals (Fig. 4, panels -5.0 and -5.5). However, the dorsal crossing fibers of the SQ-EAS and the EAS-M, which cannot be separated in the axial plane, are distinct in the coronal scans (Table 1 and Fig. 4, panels -6.5 to -7.0). Here again, the separation of the SQ-EAS and the EAS-M form the appearance of a double thickness of the sphincter complex.

The EAS-W does not appear as a separate structure on coronal scans. Also, although the bulk of the puborectalis muscle is easily seen in this scan plane, it is very difficult to separate the puborectalis muscle from the remainder of the EAS complex (Fig. 4, panels -4.0 to -5.5).

The sagittal scan plane shows the fiber direction of the external anal sphincter (Table 1, Fig. 5, panels R1.0, L1.0). Dorsally, some fibers of the EAS-M and SQ-EAS can be seen projecting toward the coccyx (Fig. 5, panels R0.5 to L0.5). Also, the separation of the SQ-EAS and the EAS-M by the ESS can easily be seen in the parasagittal slices (Table 1, Fig. 5, panels R0.5, L0.5). Another characteristic feature that is well seen in the sagittal plane is the division of the

external sphincter from the puborectalis muscle. Often, the puborectalis muscle appears as a discreet bump cephalad to the fibers of the anal sphincter (Fig. 5, panel 0).

The 3-dimensional shape of the external anal sphincter is demonstrated in Figure 1. A simplified drawing of the 3-dimensional model is shown in Figure 2. The EAS has a complicated 3-dimensional shape because it is oblique to all orthogonal scan planes, making observations in any 1 plane limited. In the axial plane, the ventral crossing fibers of the EAS-M and the SQ-EAS can clearly be seen, but the dorsal crossing fibers cannot. In the coronal plane, the opposite is true—the dorsal crossing fibers can be seen but not the ventral. Because the patients were scanned supine with their legs together, the EAS-M has a flattened and elongated “ring” appearance.

See Table 2 for demographic information of the 50 nulliparous women whose MR images were reviewed for characteristic features of the external anal sphincter. None of the patients had significant bowel incontinence problems except rare incontinence of flatus. Thirty-nine women (78%) were still menstruating, 9 (18%) were postmenopausal and not on hormonal replacement therapy, and 2 (4%) were postmenopausal and on hormonal replacement therapy. Many of the characteristic findings of the EAS could reliably be seen in the scans reviewed (Table 3). Proportions of subjects exhibiting certain characteristics were computed and presented with confidence intervals that were calculated using the normal approximation to the binomial distribution. The dorsal crossing fibers of both the EAS-M and SQ-EAS were seen in all scans reviewed (100%). The ventral crossing fibers of both structures could also be consistently identified (94% and 90%). The winged portion could be seen in the majority of nullipara (76%) and could be visibly separated from the puborectalis muscle in 62%.

DISCUSSION

Using preestablished criteria for what constitutes separate parts of a muscle, we found 3 identifiable portions of the external anal sphincter in MR images of nulliparous women. These include a subcutaneous portion (SQ-EAS), a visibly separate deeper portion (EAS-M), and a lateral portion that has lateral winged projections (EAS-W). These subdivisions were consistently visible in MR scans made without the use of an endoanal coil. The SQ-EAS has a visible separation from the remainder of the EAS in multiple scan planes, justifying its being labeled as a distinct part. Although a separation cannot clearly be seen between the concentric portion of the EAS-M and the winged EAS-W, the fibers of the winged portion have differing fiber directions than the other portions, forming an open “U-shaped” configuration. These fibers are contiguous with the EAS but visibly separate from the puborectalis muscle, whose fibers they parallel. Because these fibers clearly have differing insertions from the remainder of the EAS, we concluded that a visible separation of the components cannot be the only the criteria for dividing the structure. Therefore, differing origins and insertions was the second criterion used for subdividing the complex. Also, the fact that the EAS-W could be seen in the majority of the scans reviewed suggests it is a valid subdivision rather than an aberrant variant. Whether the instances in which this subdivision cannot be seen represent anatomic disruptions or limitations in the imaging technique cannot be determined at this time.

The controversy surrounding anal sphincter anatomy has been well summarized and reviewed by Dalley.² Anatomists since the 1930s have characterized the external anal sphincter as a structure with 1, 2, 3, or 4 parts. The various subdivision schemes were illustrated by Oh and Kark.⁵ There is general agreement that the SQ-EAS is a separate subdivision from the rest of the external sphincter. For the remainder of the EAS, various authors including Oh and Kark and Lawson⁶ have described a “superficial” and “deep” part. This lack of consensus suggests that gross anatomic dissection of the sphincter complex can be problematic and leads to arbitrary assignment of subdivisions. Dalley² referred to the EAS as 1 continuous mass and to

recommended that the “three-part external anal sphincter be removed from gross anatomy texts . . . and be relegated to the junkyard of anatomic trivia where it may languish for the sake of the historical anatomist or the rare individual who spends time carving out the most meticulous of dissection.” We would agree that for the purposes of student cadaver dissection this is a reasonable position. However, subdividing the external anal sphincter becomes necessary when the goal is to study the effect of specific anatomic disruptions on function.

The advent of imaging technologies such as anal endosonography and earlier MR studies did not help resolve the confusion over EAS subdivisions. The divisions of the EAS are not visible on anal endosonography.⁷ Earlier MR studies used endoanal coils to improve visibility of sphincter structures. This had the disadvantage of distorting the sphincter complex. Both deSouza et al³ and Williams et al⁷ found 3 subdivisions of the EAS similar to Lawson’s⁶ observations. However, Hussain et al^{8,8} proposed that the EAS was not laminar but 1 continuous structure. These disagreements may have arisen from limited image quality of earlier MRI. With improved MR imaging, authors have consistently observed a separation in the EAS. Morren et al⁴ found 2 components of the EAS with MRI, which he refers to as the deep and a superficial component. Peschers et al¹⁰ used both MRI and cross-sectional anatomy to evaluate the sphincter. They could see a clear separation between the subcutaneous and deep external anal sphincter, which we also saw in all the studies reviewed. However, no further separations could be seen on either anatomic or MR images to further subdivide the deep portion.¹⁰ As MRI has further improved, there are structures seen that have not been observed in cadaveric specimens or earlier scans.

The differing fiber directions that we observed in the subdivisions suggest differing biomechanical functions of the parts. Both the EAS-M and the SQ-EAS are concentric structures, suggesting that they have a constrictive function to close the anal canal lumen. The winged portion of the sphincter EAS-W has a similar fiber direction to the puborectalis muscle, with decussation behind the anal canal and a ventrolateral winged portion. This suggests that when activated, the fibers pull the anal canal ventrally, thereby compressing the canal. Although there are always pitfalls in directly translating anatomic observations into clinical practice, it is interesting to note that the current techniques for anal sphincteroplasty only address the circumferential portion and not the winged portion of the external anal sphincter.

There are multiple advantages of an MRI-based anal sphincter anatomic study. It avoids the sometimes arbitrary divisions that may arise due to the process of gross anatomic dissections. The ability for multiple examiners to independently evaluate the same images allows for greater objectivity, thereby establishing valid criteria that can be used to subdivide structures. Magnetic resonance images also have the advantage of being permanent records.

Due to the oblique orientation of the sphincter complex relative to both the horizontal and vertical axes, 3-dimensional models can aid in the understanding of MR cross sections. In the axial plane, the ventral crossing fibers of the EAS-M and the SQ-EAS can be seen, but the dorsal crossing fibers cannot. In the coronal plane, the opposite is true; the dorsal crossing fibers can be seen but not the ventral. These observations may explain the disagreement among various authors regarding the integrity and the thickness of the ventral external anal sphincters. Some authors have found either a shorter⁴ or noncontiguous EAS ventrally,¹¹ whereas other authors have not.^{12,12} In both the coronal and axial planes, the relationship of the EAS-M lateral to the SQ-EAS creates the appearance of a “double thickness” that authors have commented on.^{4,8,9} What makes this study unique is the combined use of clear MRI cross-sectional anatomy and 3-dimensional modeling to evaluate anal sphincter subdivisions. Although other authors have used 3-dimensional models to study the anal sphincter, they have either not investigated subdivision anatomy¹⁴ or used fixed cadaveric specimens to generate

models.¹¹ This project lays the foundation for studying the relationship between specific disruption of the anal sphincter complex and clinical symptoms.

REFERENCES

1. Sultan AH, Kamm MA, Hudson CN, Thomas JM, Bartram CI. Anal sphincter disruption during vaginal delivery. *N Engl J Med* 1993;329:1905–11. [PubMed: 8247054]
2. Dalley AF. The riddle of the sphincters: the morphophysiology of the anorectal mechanism reviewed. *Am Surg Am Surg* 1987;1987;5353:398, 298–306.
3. deSouza NM, Puni R, Kmiot WA, Bartram CI, Hall AS, Bydder GM. MRI of the anal sphincter. *J Comput Assist Tomogr* 1995;19:745–51. [PubMed: 7560320]
4. Morren GL, Beets-Tan RG, van Engelshoven JM. Anatomy of the anal canal and perianal structures as defined by phased-array magnetic resonance imaging. *Br J Surg* 2001;88:1506–12. [PubMed: 11683750]
5. Oh C, Kark AE. Anatomy of the external anal sphincter. *Br J Surg* 1972;59:717–23. [PubMed: 5070135]
6. Lawson JO. Pelvic anatomy. II. Anal canal and associated sphincters. *Ann R Coll Surg Engl* 1974;54:288–300. [PubMed: 4833780]
7. Williams AB, Bartram CI, Halligan S, Marshall MM, Nicholls RJ, Kmiot WA. Endosonographic anatomy of the normal anal canal compared with endocoil magnetic resonance imaging. *Dis Colon Rectum* 2002;45:176–83. [PubMed: 11852329]
8. Hussain SM, Stoker J, Lameris JS. Anal sphincter complex: endoanal MR imaging of normal anatomy. *Radiology* 1995;197:671–7. [PubMed: 7480737]
9. Hussain SM, Stoker J, Zwamborn AW, Den Hollander JC, Kuiper JW, Entius CA, et al. Endoanal MRI of the anal sphincter complex: correlation with cross-sectional anatomy and histology. *J Anat* 1996;189:677–82. [PubMed: 8982844]
10. Peschers UM, DeLancey JO, Fritsch H, Quint LE, Prince MR. Cross-sectional imaging anatomy of the anal sphincters. *Obstet Gynecol* 1997;90:839–844. [PubMed: 9351775]
11. Fritsch H, Brenner E, Lienemann A, Ludwikowski B. Anal sphincter complex: reinterpreted morphology and its clinical relevance. *Dis Colon Rectum* 2002;45:188–94. [PubMed: 11852331]
12. Aronson MP, Lee RA, Berquist TH. Anatomy of anal sphincters and related structures in continent women studied with magnetic resonance imaging. *Obstet Gynecol* 1990;76:846–51. [PubMed: 2216237]
13. Fenner DE. Anatomic and physiologic measurements of the internal and external anal sphincters in normal females. *Obstet Gynecol* 1998;91:369–74. [PubMed: 9491862]
14. Cornella JL, Hibner M, Fenner DE, Kriegshauser JS, Hentz J, Magrina JF. Three-dimensional reconstruction of magnetic resonance images of the anal sphincter and correlation between sphincter volume and pressure. *Am J Obstet Gynecol* 2003;189:130–5. [PubMed: 12861151]

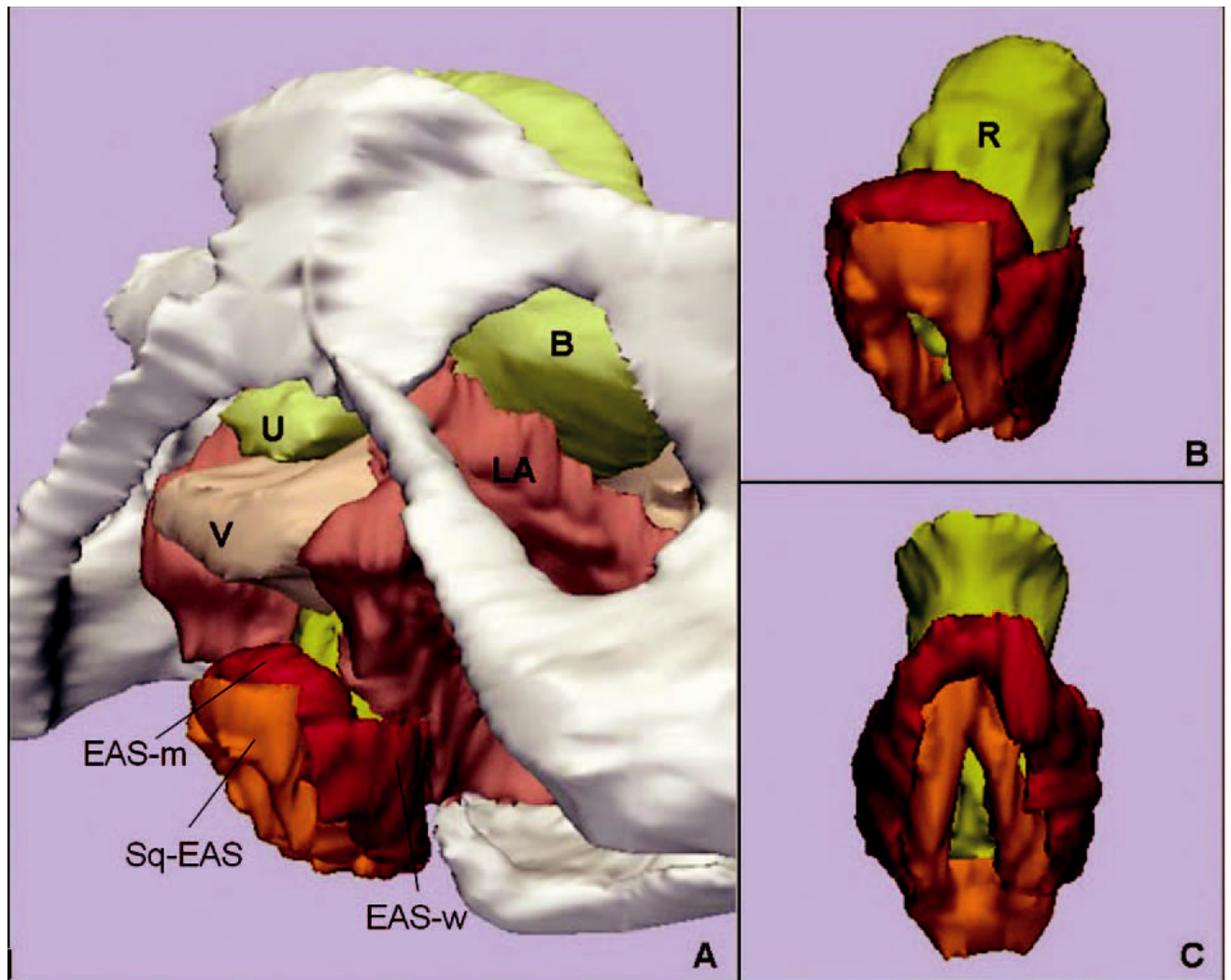


Fig. 1.

A. Inferior, left three-quarter view of model showing relationship of external anal sphincter complex to the bones and pelvic organs. **B.** Inferior, left three-quarter view of the external anal sphincter complex. External anal sphincter is in red; note the lateral wing portion of the external anal sphincter. Subcutaneous external anal sphincter is in orange. **C.** Posterior view of the external anal sphincter complex showing the circumferential nature of both the external anal sphincter and the subcutaneous external anal sphincter. U, urethra; B, bladder; V, vagina; LA, levator ani muscle; R, Rectum; EAS-M, main body of external anal sphincter; EAS-W, lateral wing portion of the external anal sphincter; SQ-EAS, subcutaneous external anal sphincter.

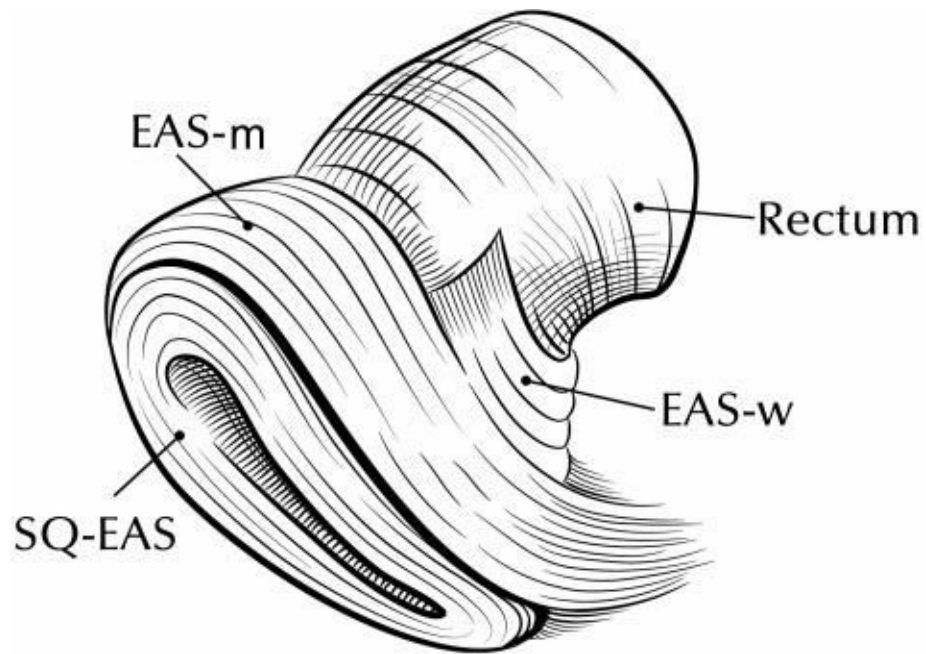


Fig. 2. Drawing of external anal sphincter (EAS) subdivisions. Anterior portion of model is to the left, posterior to the right. Notice decussation of fibers toward the coccyx posteriorly. The main body of the external anal sphincter also has a concentric portion posteriorly that is not shown in this view. EAS-M, main body of EAS; EAS-W, winged portion of EAS; SQ-EAS, subcutaneous EAS.

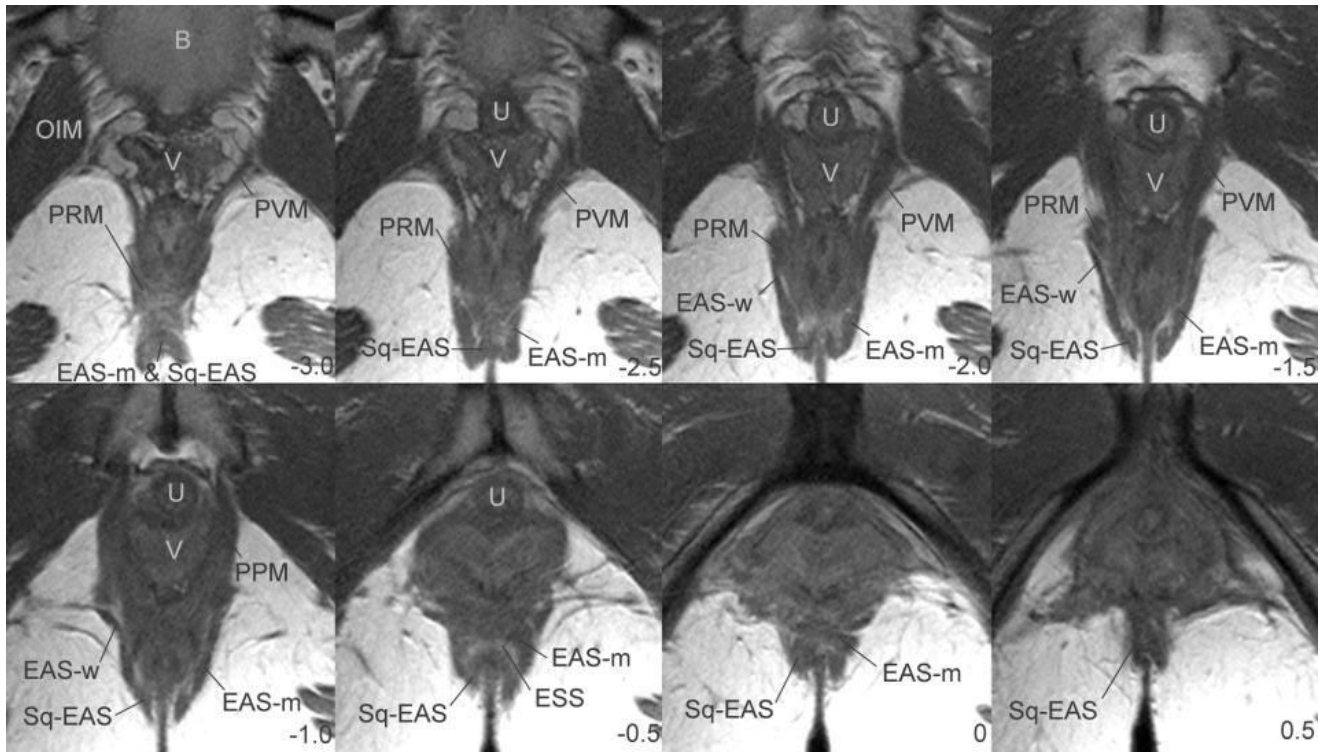


Fig. 3. Axial MRI images showing external anal sphincter anatomy. Numbering system uses the arcuate pubic ligament as reference slice (0). Slices are ordered from cephalad to caudal and are 5 mm apart. Negative numbers are cephalad, positive numbers are caudal to the arcuate pubic ligament. B, bladder; V, vagina; OIM, obturator internus muscle; PRM, puborectalis muscle; PVM, pubovisceral muscle; EAS-M, main body of external anal sphincter; U, urethra; SQ-EAS, subcutaneous external anal sphincter; EAS, external anal sphincter; EAS-W, wing portion of the external anal sphincter; P, pubic bone; PPM, puboperineus muscle; ESS, external sphincter space.

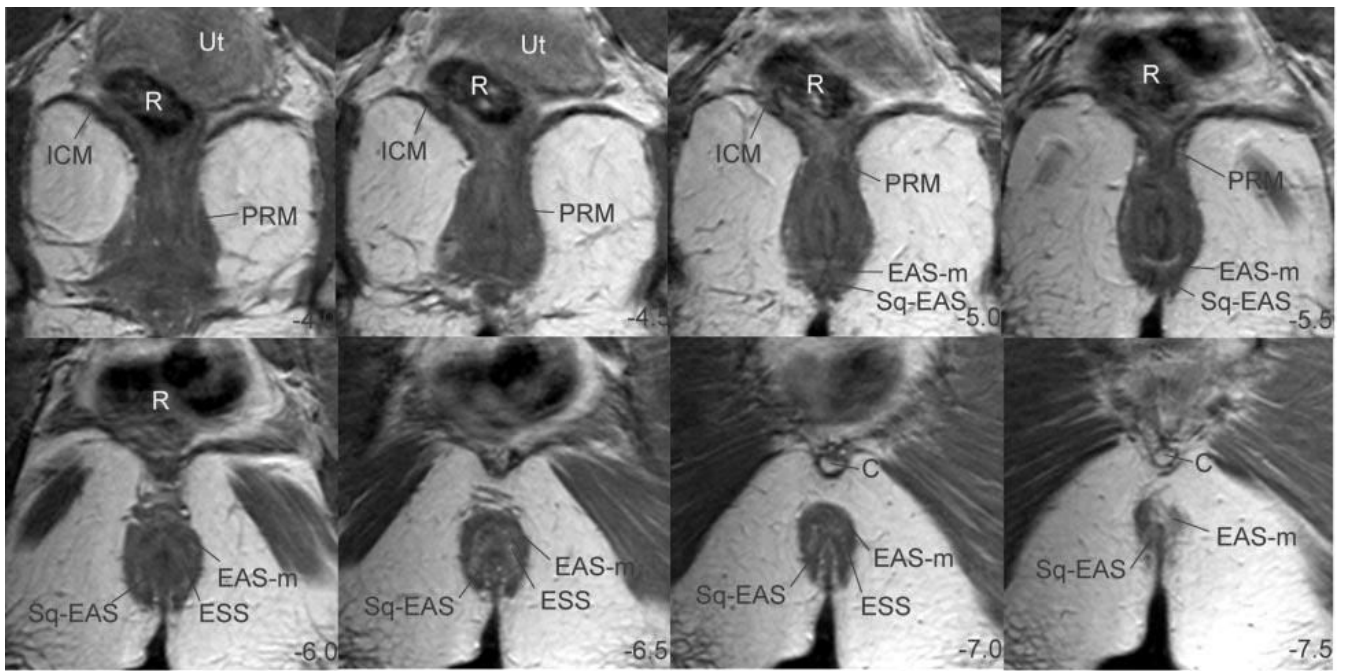


Fig. 4. Coronal MRI slices. Slices ordered from ventral to dorsal using the arcuate pubic ligament as reference. Ut, uterus; R, rectum; ICM, ileococcygeus muscle; PRM, puborectalis muscle; EAS-M, main body of external anal sphincter; EAS, external anal sphincter; SQ-EAS, subcutaneous external anal sphincter; ESS, external sphincter septum; C, coccyx.

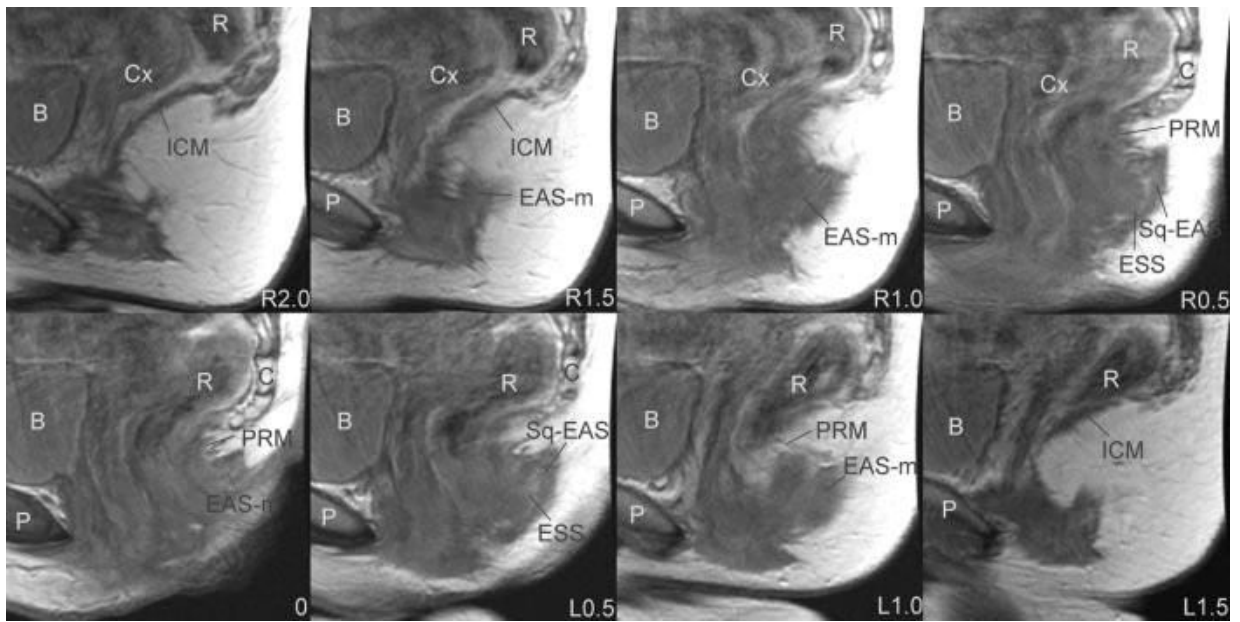


Fig. 5. Sagittal magnetic resonance imaging images. Slices are ordered from right to left using the arcuate pubic ligament as reference. P, pubic bone; B, Bladder; Cx, cervix; R, rectum; ICM, ileococcygeus muscle; EAS, external anal sphincter; EAS-M, main body of external anal sphincter; PRM, puborectalis muscle; C, coccyx; ESS, external sphincter space; SQ-EAS, subcutaneous external anal sphincter; EAS, external anal sphincter.

Table 1
Characteristic Magnetic Resonance Features of the External Anal Sphincter

	Axial (Fig. 3)	Coronal (Fig. 4)	Sagittal (Fig. 5)
EAS-M	Ventrally, crosses midline distinct from SQ-EAS (Fig 3, panels -0.5 and 0).	Dorsally, crosses midline-distinct from SQ-EAS (Fig 4, panels -6.0, -6.5, -7.0) separated by ESS.	Fiber direction oblique to horizontal and vertical axes (Fig 5, panel right 1.0)
EAS-W	Extends laterally, diverging from the midline (Fig 3, panels -2.0, -1.5, -1.0) Distinct from PRM separated by visible gap (Fig 3, panels -2.0 and -1.5)	Not possible to distinguish	Not possible to distinguish
SQ-EAS	Ventrally, crosses midline distinct from EAS-M (0.5, 0, -0.5) Adjacent to anal skin (Fig 3, panels -2.5 to -1.0)	Dorsally, crosses midline distinct from EAS-M (Fig 4, panels -6.5 and -7.0) Adjacent to anal skin (Fig 4, panels -6.5 to -7.5)	Distinct semicircle structure on parasagittal (Fig 5, panels right 0.5 to left 0.5).

EAS-M, main portion of external anal sphincter; SQ-EAS, subcutaneous external anal sphincter; ESS, external sphincter space; EAS-W, winged portion of EAS; PRM, puborectalis muscle.

Table 2

Demographic Data

	Age (y)	Body Mass Index (kg/m ²)	Maximum Prolapse Point (cm)
Mean ± standard deviation	37.3 ± 15.2	24.6 ± 5.8	-2.2 ± 0.8
Range	19-76	17.8-41.5	-3 to 0

Table 3
Frequency External Anal Sphincter Characteristic Features Seen in Nulliparous Magnetic Resonance Images

Plane	Characteristic	Visible (N = 50)
Axial	EAS-ventral crossing	47 (94 ± 6)
	EAS-wings	38 (76 ± 12)
	PRM-division	31 (62 ± 13)
Coronal	SQ-EAS-ventral crossing	45 (90 ± 8)
	EAS-dorsal crossing	50 (100)
	SQ-EAS-dorsal crossing	50 (100)
Sagittal	Distinct SQ-EAS	50 (100)
	EAS fiber direction	47 (94 ± 6)
	PRM bump	50 (100)

EAS, external anal sphincter; PRM, puborectalis muscle; SQ-EAS, subcutaneous portion of the EAS.

Values are n (%).